SENSOR LETTERS
Vol. 10, 1031–1038, 2012

Enzymatic Solid-Phase Reactor Based on Silica Organofunctionalized with *p*-Phenylenediamine for Electrochemical Detection of Phenolic Compounds

Fernando C. Moraes*, Ivana Cesarino, Diego LC Golinelli, and Sergio AS Machado

Instituto De Química De São Carlos, Universidade De São Paulo, Av. Trabalhador São-Carlense, 400, Centro, São Carlos, São Paulo, CEP 13566-590, Brasil

(Received: 6 October 2011. Accepted: 6 December 2011)

A new biomaterial, based on silica organofunctionalized with *p*-phenylenediamine (*p*-PDA) and the enzyme peroxidase, was used in the development of an enzymatic solid-phase reactor. The analytical techniques used in the characterization showed that the organic ligand was incorporated into the silica matrix. Thus, the silica modified with *p*-PDA allowed the incorporation of peroxidase by the electrostatic interaction between the carboxylic groups present in the enzyme molecules and the amino groups attached to the silica. The enzymatic solid-phase reactor was used for chemical oxidation of phenols in 1, 4-benzoquinone that was then detected by chronoamperometry. The system allowed the analysis of hydroquinone with a detection limit of 83.6 nmol L^{-1}. Thus, the new material has potential in the determination of phenolic compounds river water samples.

Keywords: *p*-Phenylenediamine, Enzymatic Solid-Phase Reactor, Phenolic Compounds.

1. INTRODUCTION

Phenol and other phenolic compounds are recognized as a major cause of soil and groundwater contamination in industrialized areas. Waste from oil refineries, ceramics and pharmaceutical industries, resins and plastic factories, among others, have been reported as potential sources of environmental contamination.[1] In this regard several chromatographic and non-enzymatic methods have been described for determination of phenolic compounds.[2–4] Biosensors based on peroxidase or polyphenoloxidases enzymes have been also widely used in the determination of phenolic compounds.[5–6]

Horseradish peroxidase and polyphenoloxidases (laccase or tyrosinase) have the ability to catalyze the oxidation of phenols, substituted phenols, and benzenediols to quinones or radical species.[7] However, the major challenge in the development of the biosensor is the enzyme immobilization. Thus an interesting strategy is the immobilization of the enzyme in a solid-phase reactor coupled in a flow system. Such combination allows an increase in sampling rate, minimize the reagents consumption, and increase the sensitivity of the analysis due to the pre-concentration effect.[8] One of the potential drawbacks is the requirement of on strong immobilization of the enzyme.

In 1992, Beck et al., described the advantages of using the mesoporous materials with ordered pores.[9] Since then, a large amount of research has been performed into synthetic methods and applications of mesoporous materials in order to control their ordered nanostructure and morphologies.[10–16] Such silica based materials have high specific surface area and mesopores with uniform size distribution, a morphology that is fundamental for many applications.[17–18] In order to combine a high surface area and a narrow pore size distribution with the advantage of owing organic ligand properties, the functionalization of porous silica surfaces has received much attention. These modifications have the potential to expand the range of applications of mesoporous silica in catalysis, sensing, and separation.[19–21] Among differences derivatization procedures, aminosilica is a type of organic/inorganic hybrid material created by incorporation of amino groups in the silica structure via synthesis or via immobilization of amino substances.

Cagnol et al.[22] reported a general route for the direct synthesis of functionalized cetyltrimethylammonium bromide (CTAB) templated silica thin films, using organotrialkoxysilanes, differing by their physical-chemical

*Corresponding author; Email: fcmoreas@hotmail.com

properties. Brinker's group.[23] used a one-pot method to prepared ordered aminopropyl functionalized silica thin films as pH sensors. Walcarius.[24] presented extensive review about the preparation and application of mesoporous organo-silica modified electrodes showing their importance as electroanalytical sensors. Due to the importance of these materials, our research group aims to develop solid-phase reactors fabricated by organofunctionalized silica with amino groups, *p*-phenylenediamine (*p*-PDA). The final goal is to prepare a reactor to be used in flow system for analysis of phenolic compounds.

This work describes a one-step synthesis of organofunctionalized silica, templated with CTAB, using *p*-phenylenediamine (*p*-PDA) as a modifier. The silica organofunctionalized with *p*-PDA was then used in the development of an enzymatic solid-phase reactor for the electrochemical detection of total amount of phenolic compounds in river water sample.

2. EXPERIMENTAL DETAILS

2.1. Instrumentation

Elemental analysis (C, H, N) was performed in a EAGER-200 apparatus (CE Instruments). Infra-red (IR) spectra were obtained in self-supported pellets in a Nicolet 5SXC spectrometer in the 1300–2000 cm^{-1} range. X-ray diffraction (XRD) patterns were recorded in a Rigaku Rotaflex Diffractometer model RU200B at 50 kV and 100 mA, using a wavelength Cu K_α radiation ($\lambda = 1.542$ Å).

Thermogravimetric curves were recorded in a TGA-951 modulus (TA Instruments) using 7 mg of sample in a platinum crucible at 10 °C/min heating rate, under air dynamic atmospheres (flow 100 mL/min).

Flow injection analysis were carried out using a model IPC 8-channel Ismatec (Zurich, Switzerland) peristaltic pump supplied with Tygon tubing. The manifold was constructed with polyethylene tubing (0.8 mm i.d.). All the reference solutions were manually injected into the carrier stream using a laboratory-constructed three-piece injector-commutator.[25] As previously described, the injector was fabricated on Perpex® and included with two fixed side bars and a sliding central bar, which is moved for sampling and injection.

Spectrophotometric measurements were carried out using a UV/visible Spectrophotometer, Cary 50 scan (Varian INC, Palo Alto, CA), provided with quartz cells of 1.0 cm path length and 4.40 mL capacity.

Amperometric experiments were performed using a model PGSTAT 30 Autolab electrochemical system (Metrohm Autolab, Utrecht, Netherlands) coupled to a personal computer and controlled with GPES 4.9 software.

2.2. Reagents and Solutions

All chemicals were of analytical grade and were used without further purification. Solutions were prepared with water purified in a Millipore Milli-Q system (resistivity ≥ 18 MΩ cm). Tetraethoxysilane 95% (TEOS, Acros Organics, USA), cetyltrimethylammonium bromide 98% (CTAB, Vetec, Brazil), *p*-phenylenediamine (Sigma-Aldrich, Germany), ethanol 99.5% (Synth, Brazil) and HCl 37% (Baker, Netherlands) were used for the synthesis of the organofunctionalized mesoporous silica, see below. Horseradish peroxidase type II (HRP) (Sigma-Aldrich, Germany) was used to modify the silica mesoporous reactor. The enzyme concentration was 200 units mg^{-1}. A 1.0×10^{-4} mol L^{-1} solution of hydroquinone (HQ) (99.8% purity, Sigma-Aldrich, Germany), was daily prepared in purified water. Aliquots of this stock solution were diluted in aqueous electrolyte solution for the UV/vis and electrochemical experiments. Solutions of sodium phosphate buffer (PBS) of ionic strength 0.1 mol L^{-1} (pH 6.0) were used in all experiments as supporting electrolyte.

2.3. Preparation of the Silica Organofunctionalized with *p*-PDA

The modified silica was synthesized by heating a mixture of 1.87 g of TEOS, 0.208 g of *p*-PDA, 5.5 g of ethanol (EtOH), 0.5 g of water and 0.4 g of a 0.1 mol L^{-1} HCl solution, at 70 °C for 1 hour. Next 0.78 g of CTAB dissolved in 10 g of EtOH were added and stirred for 1 hour at room temperature.[26] To remove the surfactant, the product was refluxed in a 1.0 mol L^{-1} HCl ethanol solution for 24 h. When preparing silica in the absence of surfactant template, the resulting deposit was microporous and no ordered, illustrating the importance of the template approach. Finally, the modified silica was filtered and washed successively with N,N'-dimethylformamide, for elimination of the excess of *p*-PDA, and then the modified silica was dried at 60 °C.

2.4. Preparation of Solid-Phase Reactor Containing HRP

The solid-phase reactor (SPR) was prepared by packing the modified silica in a polyethylene tube (100 mm long and 2.0 mm i.d.) with one end plugged with glass-wool to prevent the packing material escaping from the reactor. After the packaging step, a flow of 200 units mg^{-1}. HRP solution was passed through the SPR for 5 minutes, in order to immobilize the enzyme inside the reactor. The enzyme immobilization occurs by electrostatic interaction between carboxylic groups present in the enzyme and amino groups anchored to the silica. As described by Mora et al. these interactions are critical for the enzyme immobilization.[27]

2.5. Flow Injection System

The solid phase reactor (SPR) was inserted in the flow injection system between the injection unit (IU) and the

electrochemical flow cell (EFC) as schematically shown in Figure 1(A). Initially, the EFC worked in a stream of PBS at pH 6.0 was used as the carrier solution (carrier) at a flow rate of 3.8 mL min^{-1}, with until the baseline had reached a steady-value. Next, HQ sample contained in the sample loop (L, 100 μL) was injected and transported into the EFC. The distance from the solid phase reactor to the detector was 30 cm. This distance was selected as a compromise between 10 and 50 cm. The EFC consisted of a glassy carbon as working electrode (WE), a platinum disk as a counter electrode (CE), and an Ag/AgCl used as reference electrode (RE), as showed in Figure 1(B). The electrochemical measurements were performed by chronoamperometry using $E_{fixed} = -0.2$ V. For UV/vis measurements, aliquots of the carrier solution and hydroquinone were collected after they passed through the enzymatic SPR.

2.6. Recovery Experiments

The standard addition method was used to test the developed methodology in spiked river water. For this purpose, river water samples were spiked with 1.0 μmol L^{-1} of phenolic compounds (hydroquinone, catechol, resorcinol, and phenol) and the amperometric transient signals recorded. After that, three additions of equal amounts of phenolic compound solution were performed up to a final phenolic compounds concentration of 3.0 μmol L^{-1}. Extrapolation of the resulting linear regression plot gave the recovery amount of total phenols in the spiked river water samples.

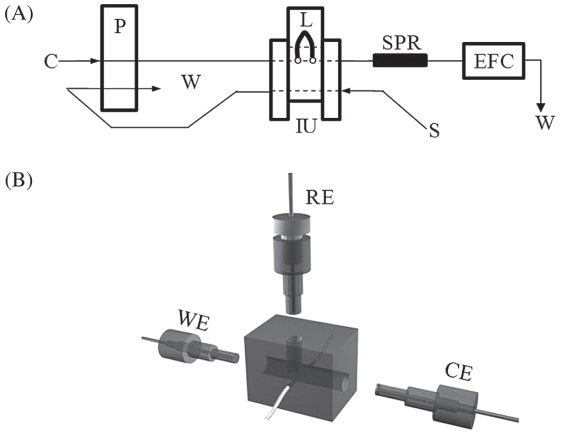

Fig. 1. (*A*) Schematic diagram of the flow injection system used for chronoamperometric determination of hydroquinone. (IU) injection unit; (*P*) peristaltic pump, (*S*) sample or reference solutions, (*L*) sample loop, (*C*) carrier solution (PBS at pH 6.0 and flow rate at 3.8 ml min^{-1}, (SPR) solid-phase reactor with 100 mm long and 2.0 mm i.d., (EFC) electrochemical flow cell and (*W*) waste. (*B*) Schematic diagram of electrochemical flow cell, polarized at −0.2 V versus Ag/AgCl. (WE) glassy carbon electrode as work electrode, (CE) platinum disk as counter electrode and (RE) Ag/AgCl as reference electrode.

2.7. HPLC Measurements

The HPLC measurements were carried out using a model Prominence LC 20 AT (Shimadzu, Kyoto–Japan), with a spectrophotometric UV/vis detector. The chromatographic column was a Phenomenex Luna C-18 (250 × 4.6 mm i.d.; 5 mm), coupled to a pre-column Supelcosil C-18 (4 × 3.0 mm i.d.; 5 mm).

The analytical curves were obtained by the standard addition method and measurements were performed in triplicate. For phenolic compounds, the mobile phase consisted of a mixture of water and acetonitrile in the following gradient mode: 0–14 minutes, 15% of acetonitrile; 14–23 minutes, 60 to 100% of acetonitrile; 23–40 minutes, 15% of acetonitrile. The oven temperature was 35 °C, with a flow rate of 0.8 mL min^{-1}, the injection volume was 20 μL, and the working wavelength for quantitative analysis was 270 nm.

3. RESULTS AND DISCUSSION

3.1. Synthesis and Characterization of Silica Organofunctionalized with *p*-PDA

The organofunctionalized silica was characterized by IR spectroscopy, thermogravimetry (TG), elemental analysis (EA), X-ray diffraction (XRD). As previously stated, cetyltrimethylammonium bromide was used as surfactant. Several studies in the literature have described how surfactant and non-aqueous co-solvents can be used to define mesophase structure.[28–29] Also that, when preparing the silica in the absence of a surfactant template, the result was only a microporous and non-ordered silica. In all cases, after the formation of mesoporous silica, the surfactant should be extracted, to avoid large increases in mass transport rates into the silica porous. Additionally the extraction imparted high accessibility to the organic moieties of organofunctionalized mesoporous silica.[30]

The results of elemental analysis obtained for the mesoporous silica synthesized in the presence and absence of amino ligand, are presented in Table I. These results revealed significant changes in the content of each element after each functionalization step. In the EA were analyzed the unmodified mesoporous silica containing the surfactant (MS-CTAB), the silica organofunctionalized with *p*-PDA

Table I. Elemental analysis (%) and number of mol for each element per 100 grams (n) of the mesoporous silica (MS-CTAB), silica organofunctionalized with *p*-PDA in the presence of surfactant (PDAS-CTAB) and after surfactant extraction (PDAS).

	N		C		H	
Sample	%	n	%	n	%	n
MS-CTAB	2.18	0.16	31.18	2.60	6.70	6.65
PDAS-CTAB	7.89	0.56	60.84	5.07	10.60	10.52
PDAS	0.36	0.03	2.13	0.18	3.09	3.06

in the presence of surfactant template (PDAS-CTAB), and the silica organofunctionalized with *p*-PDA after surfactant extraction (PDAS). EA presented an increase in the nitrogen, carbon and hydrogen contents after functionalization with *p*-PDA and suggested that the modifier is being incorporated into the silica matrix. As expected the percentage in N, C, and H was observed a decrease when the surfactant was removed.

The carbon content was used to estimate the number of mols of modifier per 100 g of silica (n) in each case. Calculations performed on the basis of the carbon percentage indicated that 0.18 mols of the modifier per 100 g of silica were observed after the surfactant extraction (PDAS). The C/N ratio of 6 for PDAS is consistent with a mixture of PDAS-CTAB (C/N 9) and PDAS (C/N 3), showing that not all of CTAB was extracted.

The Figure 2 presents the IR spectra of mesoporous silica (*a*), silica organofunctionalized with *p*-PDA in the presence of surfactant (*b*) and after surfactant extraction (*c*). The band around 3440 cm^{-1} could be attributed to the adsorbed water and to the H-bonded silanol OH groups. IR spectra of surfactant (CTAB) aggregates presented a band at 2854 cm^{-1} due to the CH_2 symmetric vibrations.[31] It is noted that the silica functionalized with *p*-PDA after surfactant extraction this band does not appear. Other bands between 1200 and 500 cm^{-1} are associated with Si–O–Si or Si–OH band vibration of the siliceous framework, e.g., 1080 cm^{-1} band with the Si–O–Si asymmetric bond stretching vibration and 960 cm^{-1} band with the Si–OH bond stretching vibration. The amino groups of *p*-PDA are indicated spectrally by a significant decrease in the intensity of the 960 cm^{-1} band.[32] Additionally, the presence of amino groups (curve c) was confirmed by a broad band extending from 3600 to 3900 cm^{-1} corresponding to the stretching vibration of N–H and also in curves *b* and *c*, one peak at 1630 cm^{-1} due to the symmetric bending vibration of $-NH_2$.

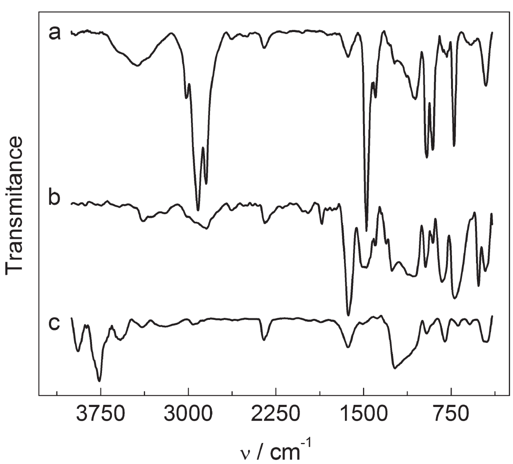

Fig. 2. IR spectra for: (a) unmodified mesoporous silica (MS-CTAB), (b) silica organofunctionalized with *p*-PDA in the presence of surfactant (PDAS-CTAB) and (c) after surfactant extraction (PDAS).

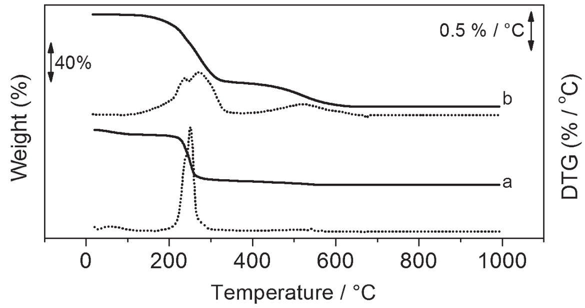

Fig. 3. TG curves for (a) non-modified silica and (b) silica organofunctionalized with *p*-PDA in the presence of surfactant. (Solid line) weight and (dotted line) derivation weight.

TG (thermogravimetry) was employed for accompanying the thermal behavior of the products obtained in the organofunctionalization. Figure 3 presents the thermogravimetric curves of mesoporous silica (curve *a*), silica organofunctionalized with *p*-PDA in the presence of surfactant (curve *b*). The MS-CTAB and PDAS-CTAB presented dehydration at the beginning of the TG curves. However the mass losses are not stoichiometric. In order to compare the mass losses in the samples the decomposition steps were normalized by discounting the dehydration process and considering the dried material as the starting mass. The MS-CTAB presents a second transition from 249–320 °C with a mass loss of *c.a.* 52.7% and a last transition with a mass loss equivalent to 5.9%. The PDAS-CTAB presents a thermal event at 161–371 °C with a mass loss of *c.a.* 70.0% and another from 371–798 °C with a mass loss of *c.a.* 24.3%. The decomposition profiles in the region of the organic matter burning are different, showing that the modifier promoted changes in the silica.[33]

The Figure 4 shows the XRD pattern for mesoporous silica with and without modification. The unmodified silica displayed a well-resolved pattern with a diffraction peak at 6.74° and two weak peaks at 10.1° and 13.6° with

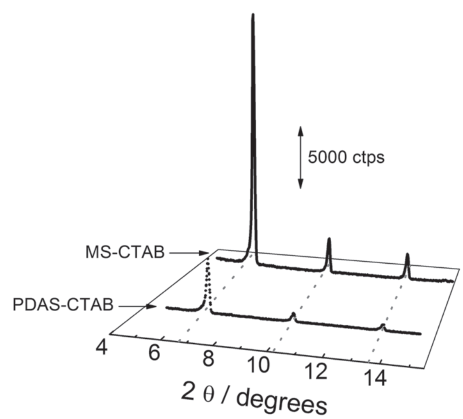

Fig. 4. XRD patterns for mesoporous silica (MS-CTAB) and silica organofunctionalized with *p*-PDA in the presence of surfactant (PDAS-CTAB).

d-spacing values of 13.10, 8.73 and 6.52 Å, respectively. After organofunctionalization with *p*-PDA a considerable decrease in the XRD peaks intensity was observed, providing further evidence of functionalization occurring mainly inside the mesopore channels. Collectively, the XRD pattern of the silica organofunctionalized also suggest not only a significant degree of short range structure ordering and well-formed hexagonal pore arrays of the samples, but also the maintenance of the structural order of the synthesized materials after functionalization.[34]

The characterization results discussed above allowed proposing a mechanism for the silica organofunctionalization, as shown in Scheme 1. This proposed mechanistic was in agreement with Wang et al. which described the architecture of a hybrid mesoporous material.[35]

3.2. Study of Enzymatic Solid-Phase Reactor Functionality

The mesoporous silica organofunctionalized with *p*-PDA was then used to construct an enzymatic solid-phase reactor (SPR). This device was integrated with a FIA system and was used for the chemical transformation of hydroquinone to an easily detectable product. The SPR preliminary study was carried out using the UV/vis absorption measurements with the spectra collected in a wavelength region between 200 to 500 nm. A solution containing 1.0×10^{-5} mol L^{-1} of HQ was passed through the enzymatic SPR, reacted with the enzyme HRP, in a oxidation reaction, forming 1,4 benzoquinone (1,4-BQ) and the spectra was shown in Figure 5. In order to compare, a spectrum of a standard solution of 1.0×10^{-5} mol L^{-1} of 1,4-BQ was performed.

It can be observed that the HQ spectrum (■) has an absorption maximum in wavelength at 280 nm. After 1.0×10^{-5} mol L^{-1} of HQ was injected into the FIA system and passed through the enzymatic SPR, an UV/vis spectrum of the product was made and the spectrum of the product (o) showed a remission of the band at 280 nm and the appearance of a band in wavelength at 405 nm. This behavior is in agreement of the study related by Kettle and Winterbourn which showed that HRP enzyme oxidized the hydroquinone forming a 1,4-benzoquinone.[36]

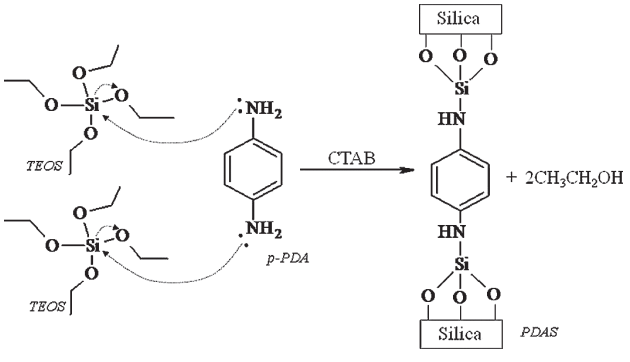

Scheme 1. Proposed mechanistic of TEOS organofunctionalized with *p*-PDA.

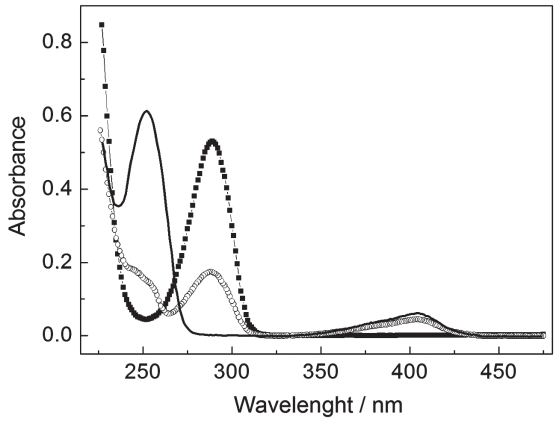

Fig. 5. Absorption spectra of 1.0×10^{-5} mol L^{-1} of hydroquinone (/), 1.0×10^{-5} mol L^{-1} of 1,4-benzoquinone (solid line), and after passage of hydroquinone through the enzymatic SPR (O).

3.3. Flow Injection System and Electrochemical Conditions

The flow injection system studies were carried out using the manifold was shown in Figure 1, aiming to optimize the reaction between the phenolic compound and the enzymatic SPR. The variables as enzyme concentration, time o enzyme solution recirculation, sample volume, flow rate, reactor length and applied potential were investigated.

The concentration of enzyme passed through the SPR was optimized in the range of 25 to 200 units mg^{-1}. The current peak of the enzymatic product formed increased, for more negative values, up to 200 unit mg^{-1} of the enzyme on SPR. The time of the enzyme recirculation was also investigated in the range of 1 to 10 minutes. The maximum value observed was in 5 minutes. For values higher than 5 minutes the analytical signal was kept constant. For this, a concentration value of to 200 unit mg^{-1} of the HRP and 5 minutes of recirculation were chosen for further experiments.

The study of the applied potential in the chronoamperometric determination of the phenolic compound was based on electrochemical behavior of the enzymatic reaction product, i.e., 1,4-BQ, on glassy carbon electrode. The cyclic voltamograms were recorded in 0.1 mol L^{-1} of PBS (pH 6.0) containing 1.0×10^{-4} mol L^{-1} of 1,4-BQ with scan rate of 50 mV s^{-1}, as shown in Figure 6.

The cyclic voltamogram of the 1,4-BQ on glassy carbon electrode surface showed a well-defined redox couple of peaks ($E_{pa} = +0.325$ V and $E_{pc} = -0.082$ V). This results are in agreement with Bowers and Yenser,[37] which related that the 1,4-BQ can be easily reduced in −0.1 V on glassy carbon electrode surface in a reaction involving 2 protons and 2 electrons. Thus, −0.2 V was chosen as the applied potential value in the chronoamperometric experiments.

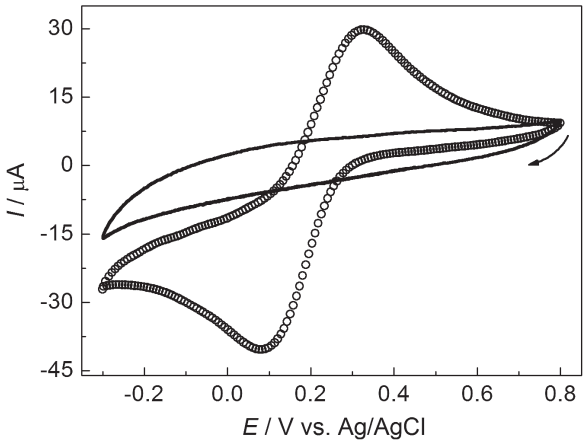

Fig. 6. Cyclic voltammograms for glassy carbon electrode in 0.1 mol L^{-1} of PBS in absence of 1,4-BQ (solid line) and presence of 1.0×10^{-4} mol L^{-1} of 1,4-BQ (◯).

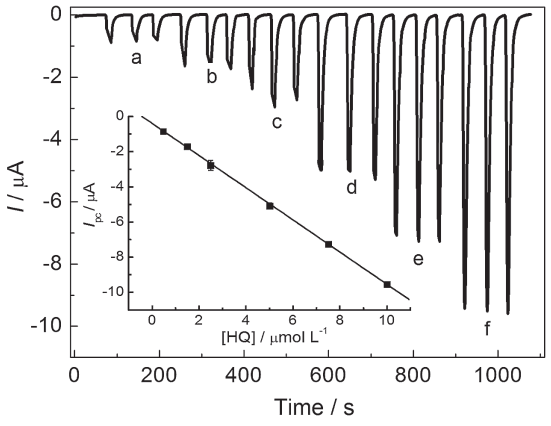

Fig. 7. Transient chronoamperometric signals in triplicate for reference hydroquinone solutions: (a) 0.5; (b) 1.5; (c) 2.5; (d) 5.0 (e) 7.5 and (f) 10.0 μmol L^{-1}, using $E_{fixed} = -0.2$ V, flow rate at 3.8 mL min^{-1} and sample volume of 100 μL. Inset: linear dependence of the mean of the currents with hydroquinone concentration.

The influence of reactor length on the amperometric response was studied in the 1.5 to 12 cm range at a carrier flow rate of 3.8 mL min^{-1} and 1.0×10^{-4} mol L^{-1} of hydroquinone solution passed through the SPR. The current signals increased gradually with the reactor length. However, a reactor length larger than 10 cm showed low reproducibility of the analytical signals and baseline instability. Thus, a reactor length of 10 cm was used in further experiments.

The effect of the sample from 10 to 150 μL on the analytical signal was evaluated by injection of 1.0×10^{-4} mol L^{-1} of hydroquinone solution in 0.1 mol L^{-1} of PBS (pH 6.0) at a carrier flow rate of 3.8 mL min^{-1}. The current increased with the increase of sample volumes from 10 to 100 μL and it was kept constant in sample volume until 150 μL. Therefore, a sample volume 100 μL was selected for showing better relation between sensibility and analytical frequency. The effect of flow rate from 0.5 to 5.0 mL min^{-1} over the analytical signal was studied and the optimal flow rate found was 3.8 mL min^{-1} over.

3.4. Figures of Merit

Using the conditions optimized according to the experiments described in flow injection system and electrochemical conditions section, a chronoamperometry was used to investigate the electrochemical response as a function of the hydroquinone concentration. A set of reference solutions of HQ were injected into the flow injection system, in triplicate. I all cases, transients signals corresponding to 1,4-BQ produced from oxidation process of HQ by the enzymatic SPR were obtained. The analytical response shown in Figure 7 has a linear range of 0.5–10.0 μmol L^{-1}, according to:

$$I(\mu A) = -0.38 \pm 0.02(\mu A) - 0.92 \pm 0.04(\mu A/\mu \text{mol L}^{-1}) \times [HQ](\mu \text{mol L}^{-1})$$

with a correlation coefficient of 0.999 ($n = 6$). The LOD of 83.6 nmol L^{-1} was determined using a 3σ/slope ratio, where σ is the standard deviation of the mean value for 10 chronoamperograms obtained upon injections of PBS, according to IUPAC recommendations.[38]

The reproducibility of SPR was measured in 10 different experiments ($n = 10$) on 3 different days with a different SPR in each day. Prior to each experiment, a flow of PBS was passed SPR. Thus, seven injections of 1.0×10^{-4} mol L^{-1} of hydroquinone were made and the chronoamperograms were collected. The relative standard deviation (RDS) was calculated in 2.7% ($n = 30$). The repeatability tests were performed in 10 different chronoamperograms with the same concentration of HQ and the RDS was found to be 1.7% ($n = 10$). An analytical frequency of 65 determinations per hour was measured.

The shelf life of the enzymatic SPR was evaluated by measurements repeated several times, each day, and after 30 days the device had lost only 6.7% of its functionality, therefore the enzymatic SPR can be used for at least one month when stored in 0.2 mol L^{-1} PBS pH 7.0 at 4 °C. The life time was at least over 300 determinations indicating the high stability of this device.

Messina et al. developed one method based in an enzymatic rotating bioreactor for determination of ascorbic acid (Messina et al. 2004) and another method based in an online microfluidic sensing device with an enzyme-modified pre-cell coupled to an amperometric detector for the monitoring of paracetamol (Messina et al. 2006). The first system allowed the analysis of L-ascorbic with a detection limit of 6.0 nmol L^{-1} in the processing of as many as 25 samples per hour. The second method determined paracetamol with a limit of detection of 0.3 μmol L^{-1} in the processing of as many as 20 samples per hour. Comparing these two methods with the bioreactor proposed in this work the great advantage of the enzymatic SPR is

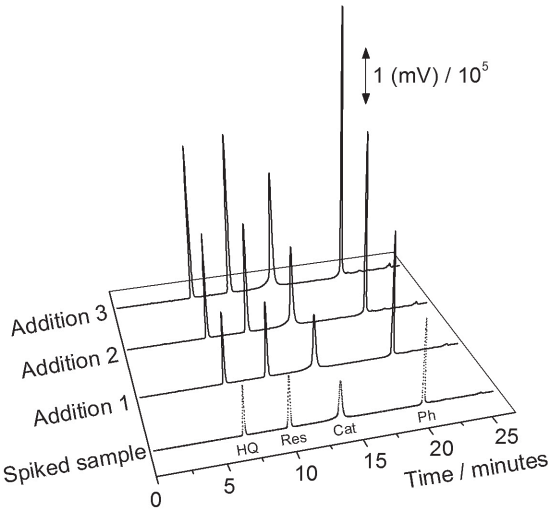

Fig. 8. Chromatograms for river water sample. Sample spiked with 1.0 μmol L^{-1} of the phenolic compounds mixture (dotted line). Additions of the phenolic compounds mixture standard (solid line): Addition 1 (2.0 μmol L^{-1}); Addition 2 (2.5 μmol L^{-1}); Addition 3 (3.0 μmol L^{-1}).

the analytical frequency (65 determinations per hour) and the high stability.

3.5. Analysis of Total Amount of Phenolic Compounds in River Water

The proposed enzymatic SPR was applied to the analysis of the phenolic compounds in river water, using the standard addition method, in order to eliminate any matrix effects. For this purpose, a polluted water sample with a high content of organic components was collected in São Carlos (SP/Brazil). The samples of river water, collected from the river, were directly used (without any treatment) in the preparation of the 0.1 mol L^{-1} of PBS pH 6. After, 3 samples of river water were spiked with 1.0 μmol L^{-1} of a mixture of phenolic compounds (hydroquinone, catechol, resorcinol, and phenol). The average results obtained using the standard addition method, for 3 determinations, for each sample, were: 0.95, 0.98 and 1.02 μmol L^{-1} of total phenols. Recoveries between 95.0 and 102% of phenolic compounds from river water samples ($n = 3$) were obtained.

Table II. Determination of total amount of phenolic compound in river water sample (each value is the mean of three determinations).

	Proposed enzymatic SPR			HPLC	
	Spiked (μmol L^{-1})	Found (μmol L^{-1})	Recovery (%)	Found (μmol L^{-1})	E_r^* (%)
Sample 1	1.0	0.95	95	0.99	−0.42
Sample 2	1.0	0.98	98	1.00	−1.01
Sample 5	1.0	1.02	102	0.99	+2.94

Note: *Er = Detected proposed enzymatic SPR versus Detected HPLC.

In order to compare the results obtained with the proposed enzymatic SPR method, HPLC experiments were performed to analyze the total amount of phenolic compounds in river water. The samples of river water tested were prepared spiking a mixture of hydroquinone (HQ), resorcinol (Res), catechol (Cat), and phenol (Ph), in which the final concentration of total phenols was 1.0 μmol L^{-1}.

The Figure 8 shows the chromatograms obtained for the river water sample spiked with phenolic mixture and the addition of several concentrations of the phenolic mixture. The retention times were found to be 6.4 minutes for hydroquinone, 9.8 minutes for resorcinol, 13.4 minutes for catechol, and 19.6 minutes for phenol. Using the standard addition method, the recovery experiments were carried out and the results were summarized in the Table II. According to the Student's *t*-test, there were no significant differences between the HPLC and the biosensor methods at a 95% confidence level. The good values observed in the recovery procedure show that the proposed method is suitable and efficient for the quantitative determination of total amount of phenolic compounds in river water sample.

4. CONCLUSIONS

The analytical techniques used in the characterization showed that the *p*−phenylenediamine was incorporated into the silica matrix. The presence of the surfactant in the silica synthesis step is important to define mesoporous structure and its extraction from silica led to a high accessibility to the organic molecule of organofunctionalized mesoporous silica. The modified silica allowed the incorporation of HRP enzyme by the electrostatic interaction between carboxylic groups present in enzyme molecules and amino groups displayed on silica matrix. This biomaterial was used in the development of an enzymatic solid-phase reactor for chemical oxidation of hydroquinone in 1, 4-benzoquinone. The forming product was characterized by UV/vis and a chronoamperometric flow injection system coupled to enzymatic SPR was used to quantify hydroquinone with detection limits of 83.6 nmol L^{-1}.

Comparing the results at enzymatic SPR with other electroanalytical methods, the use of a biosensors for determination of hydroquinone described,[39–40] has a higher detection limit of 8.30 μmol L^{-1} and 8.10 μmol L^{-1} respectively. Using a PVC-graphite composite electrode,[41] a lower detection limits reaching 45.0 nmol L^{-1} was found. However, for the enzymatic SPR, high lifetime and analytical frequency, good reproducibility and simple instrumentation, preparation and analytical procedure are important advantages. The results obtained by the proposed methodology for total amount of phenolic compounds in river water sample were quite similar to those obtained using the HPLC procedure. This method can be easily applied to the determination of other phenolic compounds in environmental samples and presents great

potential in the fields of electroanalytical and biosensing applications.

Acknowledgments: Financial support from the FAPESP (Processes 2010/11049-2 and 2010/11567-3) is gratefully acknowledged.

References and Notes

1. J. Arana, E. T. Rendon, J. M. D. Rodriguez, J. A. H. Melian, O. G. Diaz, and J. P. Pena, *Chemosphere.* 44, 1017 (**2001**).
2. A. L. Sun, J. Li, and R. M. Liu, *J. Sep Sci.* 29, 995 (**2006**).
3. C. H. Lin, J. Y. Sheu, H. L. Wu, and Y. L. Huang, *J. Pharm. Biomed. Anal.* 38, 414 (**2005**).
4. F. C. Moraes, S. T. Tanimoto, G. R. Salazar-Banda, S. A. S. Machado, and L. H. Mascaro, *Electroanalysis* 21, 1091 (**2009**).
5. O. D. Leite, K. O. Lupetti, O. Fatibello, I. C. Vieira, and A. D. Barbosa, *Talanta* 59, 889 (**2003**).
6. R. S. Freire, S. Thongngamdee, N. Duran, J. Wang, and L. T. Kubota, *Analyst.* 127, 258 (**2002**).
7. R. S. Freire, N. Duran, and L. T. Kubota, *Talanta* 54, 681 (**2001**).
8. L. H. Marcolino-Junior, M. F. S. Teixeira, A. V. Pereira, and O. Fatibello, *J. Pharm. Biomed. Anal.* 25, 393 (**2001**).
9. J. S. Beck, J. C. Vartuli, W. J. Roth, M. E. Leonowicz, C. T. Kresge, K. D. Schmitt, C. T. W. Chu, D. H. Olson, E. W. Sheppard, S. B. McCullen, J. B. Higgins, and J. L. Schlenker, *J. Am. Chem. Soc.* 114, 10834 (**1992**).
10. S. A. Bagshaw, E. Prouzet, and T. J. Pinnavaia, *Science* 269, 1242 (**1995**).
11. D. Y. Zhao, J. L. Feng, Q. S. Huo, N. Melosh, G. H. Fredrickson, B. F. Chmelka, and G. D. Stucky, *Science* 279, 548 (**1998**).
12. Y. Miyake, T. Yumoto, H. Kitamura, and T. Sugimoto, *Phys. Chem. Chem. Phys.* 4, 2680 (**2002**).
13. Y. Miyake and T. Kato, *J. Chem. Eng. Jpn.* 38, 60 (**2005**).
14. D. Margolese, J. A. Melero, S. C. Christiansen, B. F. Chmelka, and G. D. Stucky, *Chem. Mater.* 12, 2448 (**2000**).
15. Q. S. Huo, J. L. Feng, F. Schuth, and G. D. Stucky, *Chem. Mater.* 9, 14 (**1997**).
16. X. Feng, G. E. Fryxell, L. Q. Wang, A. Y. Kim, J. Liu, and K. M. Kemner, *Science* 276, 923 (**1997**).
17. N. Shimura and M. Ogawa, *Bull. Chem. Soc. Jpn.* 78, 1154 (**2005**).
18. S. Mann and G. A. Ozin, *Nature* 382, 313 (**1996**).
19. I. Cesarino, E. T. G. Cavalheiro, and C. M. A. Brett, *Electroanalysis* 22, 61 (**2010**).
20. I. Cesarino and E. T. G. Cavalheiro, *Electroanalysis* 20, 2301 (**2008**).
21. H. Yang, N. Coombs, I. Sokolov, and G. A. Ozin, *Nature* 381, 589 (**1996**).
22. F. Cagnol, D. Grosso, and C. Sanchez, *Chem. Commun.* 15, 1742 (**2004**).
23. H. Y. Fan, Y. F. Lu, A. Stump, S. T. Reed, T. Baer, R. Schunk, V. Perez-Luna, G. P. Lopez, and C. J. Brinker, *Nature* 405, 56 (**2000**).
24. A. Walcarius, *Electroanalysis* 20, 711 (**2008**).
25. M. F. S. Teixeira, O. Fatibello, C. Aniceto, and C. O. C. Neto, *Lab. Robotics Automat.* 11, 163 (**1999**).
26. D. Y. Zhao, P. D. Yang, D. I. Margolese, B. F. Chmelka, and G. D. Stucky, *Chem. Commun.* 22, 2499 (**1998**).
27. M. F. Mora, C. E. Giacomelli, and C. D. Garcia, *Anal. Chem.* 81, 1016 (**2009**).
28. D. Y. Zhao, Q. S. Huo, J. L. Feng, B. F. Chmelka, and G. D. Stucky, *J. Am. Chem. Soc.* 120, 6024 (**1998**).
29. Q. S. Huo, D. Y. Zhao, J. L. Feng, K. Weston, S. K. Buratto, G. D. Stucky, S. Schacht, and F. Schuth, *Adv. Mater.* 9, 974 (**1997**).
30. M. Etienne and A. Walcarius, *Electrochem. Commun.* 7, 1449 (**2005**).
31. Z. L. Hua, J. L. Shi, L. Wang, and W. H. Zhang, *J. Non-Cryst. Solids* 292, 177 (**2001**).
32. W. R. Thompson, M. Cai, M. K. Ho, and J. E. Pemberton, *Langmuir* 13, 2291 (**1997**).
33. I. Cesarino and E. T. G. Cavalheiro, *Materials Research-Ibero-American Journal of Materials* 11, 465 (**2008**).
34. D. Perez-Quintanilla, I. del Hierro, M. Fajardo, and I. Sierra, *J. Hazard Mater.* 134, 245 (**2006**).
35. J. Q. Wang, L. Huang, M. Xue, Y. Wang, L. Gao, J. H. Zhu, and Z. G. Zou, *J. Phys. Chem. C* 112, 5014 (**2008**).
36. A. J. Kettle and C. C. Winterbourn, *J. Biol. Chem.* 267, 8319 (**1992**).
37. M. L. Bowers and B. A. Yenser, *Anal. Chim. Acta* 243, 43 (**1991**).
38. Analytical Methods Committee, *Analyst.* 112, 199 (**1987**).
39. I. C. Vieira, O. Fatibello, and L. Angnes, *Anal. Chim. Acta* 398, 145 (**1999**).
40. I. C. Vieira and O. Fatibello, *Talanta* 52, 681 (**2000**).
41. F. Albertus, A. Llerena, J. Alpizar, V. Cerda, M. Luque, A. Rios, and M. Valcarcel, *Anal. Chim. Acta* 355, 23 (**1997**).